PHOTODISSOCIATION OF ROOM-TEMPERATURE AND JET-COOLED WATER AT 193 nm

Axel Ulrich GRUNEWALD, Karl-Heinz GERICKE and Franz Josef COMES
Institut für Physikalische und Theoretische Chemie an der Universität Frankfurt am Main, Niederurseler Hang, D-6000 Frankfurt am Main 50, Federal Republic of Germany

Received 20 October 1986; in final form 24 November 1986

The photodissociation dynamics of water in its first absorption band has been studied in detail by photolyzing room-temperature and jet-cooled H_2O with an ArF excimer laser at 193 nm. The fate of the ejected OH($X\,^2\Pi$) photofragments was probed by laser-induced fluorescence. The excess energy is transferred almost exclusively into translational motion of the products, $f_t = 0.97$. The rotational distribution depends strongly on the initial temperature. For warm water ($T = 300$ K), the rotational distribution can be described by a Boltzmann distribution with a temperature parameter of 400 K. No significant difference between the two Λ components, probed via Q and R, P lines, was observed. In the case of jet-cooled H_2O the rotational distribution of the Π^- component of the Λ doublets can be described by a temperature parameter of 330 K; that of the Π^+ component strongly deviates from a Boltzmann distribution. The Λ doublet population shows an increasing inversion with increasing J_{OH}. The dissociation process does not distinguish between the two spin–orbit states and the spin is only a spectator in the dissociation process of H_2O at 193 nm. These results are compared with observations of the photolysis of water at 157 nm.

1. Introduction

The photodissociation of H_2O in the first absorption band has been extensively studied in relation to the fragmentation dynamics of triatomic molecules. Recently Andresen et al. [1] reported detailed experimental results for the dissociation of water using an excimer laser at 157 nm,

$$H_2O(\tilde{X}\,^1A_1) + h\nu(157\text{ nm}) \rightarrow H_2O(\tilde{A}\,^1B_1) \rightarrow H(^2S) + OH(X\,^2\Pi, v, N, \Omega, \Lambda)\,. \quad (1)$$

The $\tilde{A}^1B_1$ excited state potential energy surface, which is involved in the fragmentation process (1), has been characterized using quantum-chemical ab initio methods by Staemmler and Palma [2]. In principle, the exit channel

$$H_2O(\tilde{A}\,^1B_1) \rightarrow H_2(^1\Sigma_g^+) + O(^1D) \quad (2)$$

is also accessible at the wavelength used (157 nm). However, the calculations show that the largest gradients of the potential energy surface are directed towards exit channel (1) and the main process will be the formation of a H atom and an OH radical, as is observed experimentally [1].

The photodissociation of vibrationally excited water molecules, prepared in a single rotational state, has also been studied [3]. The OH distributions observed depend strongly on the initially prepared quantum state of the H_2O parent. All experimental results can be almost quantitatively described by theoretical calculations [4,5].

In this paper we present results on the photofragmentation of water at 193 nm. This photolysis wavelength is at the far end of the H_2O absorption spectrum and the products ought to be exclusively $H(^2S)$ and ground-state OH($X\,^2\Pi$) radicals because exit channel (2) becomes energetically feasible only at wavelengths shorter than 176 nm [6].

The recoiling OH fragments were analyzed by laser-induced fluorescence. Due to the high spectral resolution of the applied dye laser, fine details such as spin state and Λ state populations could be studied besides the partitioning of the excess energy into the product rotational and vibrational degrees of freedom. The influence of the internal rotational temperature of the H_2O parent was investigated by cooling in a pulsed nozzle expansion.

0 009-2614/87/$ 03.50

2. Experimental

The photodissociation of H_2O was investigated in a stainless steel chamber which was evacuated by two 500 ℓ/s oil diffusion pumps. The vessel was provided with different gas inlet systems permitting the observation of the photofragmentation process in the bulk as well as in a supersonic jet. A beam of cold H_2O was produced by bubbling helium at a pressure of 20 kPa through distilled liquid water and expanding the gas mixture (20 kPa He, 2.4 kPa H_2O) through a pulsed nozzle which had a diameter of 1 mm. The displaceable commercial pulsed source (Lasertechnics) was mounted at the vacuum chamber. The total background pressure in the reaction cell was less than 0.01 Pa when the nozzle was operating at a gas pulse length of 200 μs fwhm and a repetition rate of 10 Hz. Water at room temperature was studied using a flow system with H_2O pressures of typically 1.3 Pa (10 mTorr).

The photodissociating light source (193 nm) was an ArF excimer laser (Lambda Physik EMG 200). The diverging UV beam was weakly focused into the reaction cell using a 1 m spherical dielectric mirror. At the point of observation the beam size was reduced to ≈4 mm diameter. A frequency-doubled dye laser (Lambda Physik FL 2002 E in connection with an Inrad autotracking system was used for selective probing of nascent OH fragments. The pump source of the analyzing dye laser was the second harmonic of a Nd:YAG laser (Spectron SL 2Q). The dye solution was a mixture of DCM and rhodamine 101 to provide constant output energies over a wide tuning range, which was important for an accurate comparison of the line intensities of OH originating from different vibrational levels.

With an average output energy of 5 μJ no saturation effects in the LIF detection were observed. With the aid of an intracavity etalon, the bandwidth can be reduced to 0.1 cm^{-1} in the UV. The photolysis and the probe laser beam were counterpropagated through the cell passing a series of baffles to reduce scattered light.

A homemade trigger device with four independent delay sets (jitter < 2 ns) controlled all time events in the experiment. The delay between the photolysis and the probe laser pulse was set to 50–100 ns to give the best S/N ratio.

LIF was detected at right angles to both the gas beam and the two counterpropagating laser beams by a photomultiplier tube (bialkali) equipped with imaging optics and an interference filter (310 ± 10 nm). The photomultiplier output voltage was measured with a boxcar integrator (SRS SR 250; 0.5 μs gate width) and connected to a computer, which controlled the scanning of the dye laser and normalized the fluorescence signal to the photolysis and probe laser energies for individual laser shots.

3. Results and discussion

In the photodissociation of $H_2O(\tilde{X}\ ^1A_1)$ at 193 nm, only the lowest excited electronic state, $\tilde{A}\ ^1B_1$ can be excited and the fragments are exclusively $H(^2S)$ and ground-state $OH(X\ ^2\Pi)$ radicals. The internal state distribution of the OH photoproducts was analyzed by excitation of the $X\ ^2\Pi_{3/2,1/2} \rightarrow A\ ^2\Sigma^+$ band [7–9].

The rotational distribution of the OH fragments depends on the initial rotational temperature of the H_2O parent. With warm H_2O, the rotational state distribution of the $v'' = 0$ vibrational level of OH was analyzed by fitting the data to a Boltzmann distribution. If a plot of $\ln[P(J)/(2J+1)]$ versus E_{rot} can be represented by a straight line, then we have a Boltzmann distribution which is characterized by a "rotational temperature" parameter T_{rot}. Fig. 1 shows such a plot for both spin systems ($^2\Pi_{3/2}$, $^2\Pi_{1/2}$) and for both Λ components (Π^+, Π^-). The total distribution can be described by a straight line with a temperature parameter of $T = 400 \pm 50$ K. The spin and Λ components are equally populated according to the rotational temperature. The rotational distribution of ejected fragments changes significantly when the $\tilde{A}^1B_1$ state of jet cooled H_2O (fig. 2) is excited indicating that details of the dissociation process are smeared out by the parent rotation.

We determined the influence of electron spin in the photodissociation of cold H_2O by calculating the ratio of the population numbers of the $^2\Pi_{3/2}$ and $^2\Pi_{1/2}$ states for each nuclear rotational angular momentum N, where suitable statistical weights have been used. No significant preference for one spin state could be observed. Thus, the dissociation process does not distinguish between the two spin–orbit states and the rotational population is distributed statisti-

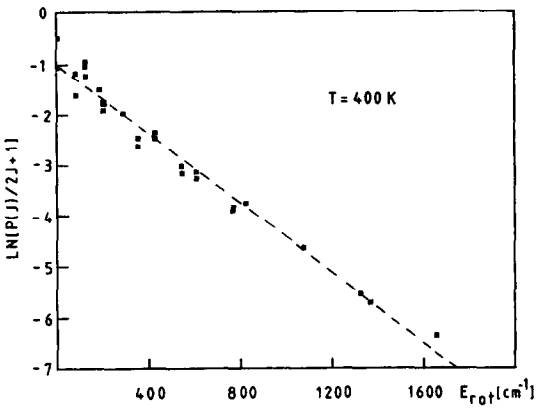

Fig. 1. Boltzmann plot of the OH($X\,^2\Pi_{3/2,1/2}$) rotational product state distribution in $v''=0$ generated by the photolysis of warm ($T=300$ K) $H_2O(\tilde{X}\,^1A_1)$ at 193 nm. The rotational distribution is characterized by a temperature parameter of $T_{rot}=400\pm50$ K for both the $^2\Pi_{3/2}$ and the $^2\Pi_{1/2}$ spin system. The experimental conditions were $P=1.3$ Pa with a 50 ns time delay between the photolysis and analysis laser pulses.

cally between the two spin components. The spin is only a spectator in the fragmentation process of H_2O at an excitation wavelength of 193 nm. As a consequence, we used a Hund's case (b) approximation and the rotational state distribution of the $v''=0$ level was analyzed by plotting $\ln[P(N)/(2N+1)]$ as a function of $B_{OH}N(N+1)$, where $B_{OH}=18.87$ cm^{-1} is the rotational constant of the OH radical [9]. Such a plot is shown in fig. 2 for both the $^2\Pi_{3/2}$ (squares) and the $^2\Pi_{1/2}$ (circles) spin systems. For a better representation, the figure is divided into two parts. The upper part shows the population numbers of the Π^- component of the Λ doublet, which for high rotations has the unpaired electron in a pπ orbital aligned parallel to the rotational vector N_{OH}. This component is probed by the Q lines while the R and P branches analyze the Π^+ component (lower part of fig. 2), which has the unpaired electron in a pπ orbital aligned perpendicular to N_{OH}. Only the rotational distribution of the Π^- component can be described by a straight line. From the slope $m=-hc/kT_{rot}$ we obtain a value for the rotational temperature parameter of $T=330\pm40$ K. The rotational temperature of OH decreases from 400 to 330 K (Π^- component) on going from room-temperature to jet-cooled H_2O. Obviously the upper potential surface has only a negligible influence on the development of OH fragment rotation.

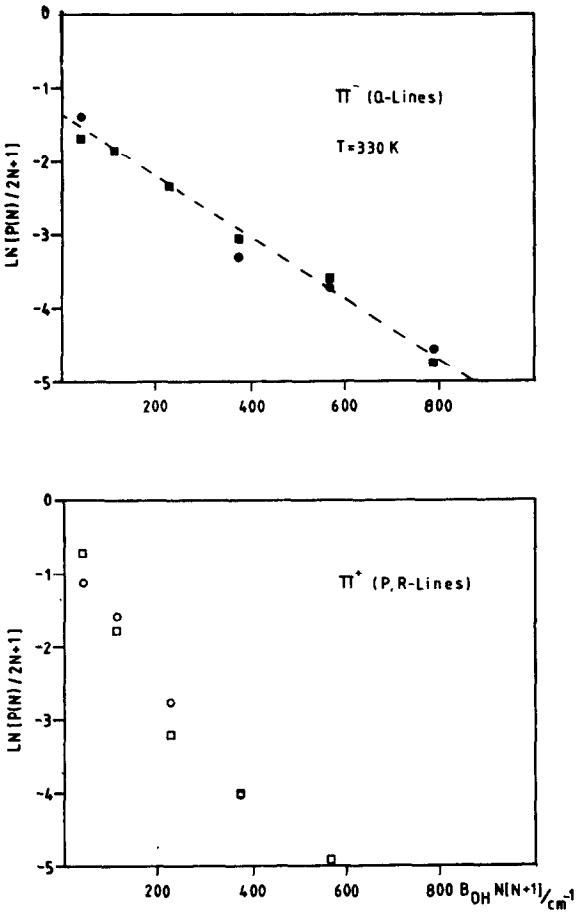

Fig. 2. OH rotational state populations $P(N)$ after dissociation of jet-cooled H_2O at 193 nm. Plotted is $\ln[P(N)/(2N+1)]$ versus $B_{OH}N(N+1)$, where N is the quantum number of the rotational motion of the nuclei and B_{OH} is the rotational constant. The rotational distribution of the Π^- component of the Λ doublet (upper part of the figure) can be characterized by a temperature parameter $T_r=330\pm50$ K. The Π^+ component (lower part) is much less populated indicating the creation of an OH fragment with an unpaired pπ lobe preferentially perpendicular to the H_2O plane.

The most striking feature in the photodissociation of cold H_2O is the strong preference for the Π^- component, which, in general, is the upper Λ component except for $N\leqslant4$ for the $^2\Pi_{1/2}$ levels. With increasing N a strongly increasing Λ-doublet inversion is found. Thus OH is ejected with an unpaired pπ lobe preferentially orientated perpendicular to the H_2O plane. The population inversion of the Λ doublets is comparable to that observed in the photolysis of H_2O at 157 nm and will, therefore, not be discussed further

[1,3,5].

The OH state distribution as given above has been determined with no corrections for alignment. In order to study the alignment of the OH photoproduct, the excimer laser light was polarized by a Rochon MgF_2 polarizer and the intensities of the $Q_1(3)$ and the $^qP_{21}(3)$ satellite lines were observed with the excimer light polarized parallel and perpendicular to the propagation direction of the analyzing dye laser beam†. The positive alignment parameter, $A_0^{(2)} = 0.4 \pm 0.1$, indicates that the OH rotational vector is preferentially aligned parallel to μ_{H_2O}, as expected in the photodissociation of H_2O.

Since the population numbers were obtained with an unpolarized photolysis laser, the alignment should not significantly affect the product state distribution. The maximum deviation in the observed intensities should be less than 5% for $A_0^{(2)} = 0.4$.

In order to detect vibrationally excited OH fragments the dye laser was scanned around 312 nm, where transitions in the $X^2\Pi(v''=1) \rightarrow A^2\Sigma(v'=1)$ band should occur. However, only absorption lines originating from the $v''=0$ level could be assigned. This is in contrast to the photodissociation of H_2O at 157 nm, where more than 50% of the OH fragments were formed in vibrationally excited states [1].

From the noise level and the signal observed in the OH transitions originating from $v''=0$ levels, we determined an upper limit for OH products formed in $v''=1$. According to this procedure, less than 3% of the fragments are vibrationally excited. This result is in agreement with ab initio calculations of the photodissociation of water where no vibrationally excited OH products are predicted for excitation above 175 nm [4]. Very recently, Engel et al. studied the partial cross section $\sigma(v''_{OH})$ of water in the first continuum by ab initio calculations [11]. The OH vibrational distribution they obtained is in good agreement with the experimental results at 157 nm. The calculations show that the vibrational excitation of the OH fragment should decrease with increasing photolysis wavelength and at 193 nm no vibrationally excited OH is expected. Additionally, examination of the calculated excited-state surface, $\tilde{A}^1B_1$, shows that, for energetic reasons, a Franck–Condon transition at 193 nm would place the molecule close to the saddle point along the symmetric stretch coordinate. Therefore, no vibrationally excited OH fragments will be formed.

The excess energy, E_{av}, which has to be distributed over the various degrees of freedom of the fragments is given by

$$E_{av} = h\nu + E_{int}(H_2O) - D_0 = 128.5 \text{ kJ/mol}, \quad (3)$$

where $D_0 = 494.1$ kJ/mol is the dissociation energy to form the products in their ground state from H_2O in its lowest state, $h\nu = 618.9$ kJ/mol (193.3 nm), and E_{int} is the internal energy of water, which is almost exclusively given by the rotational energy of the parent H_2O, $\frac{3}{2}RT_{H_2O} = 3.7$ kJ/mol. The fraction of energy released into rotation of the OH fragment, f_r, is given by

$$f_r = \langle E_r \rangle / E_{av} = 1\, RT_{OH}/E_{av}\,. \quad (4)$$

Thus, for room-temperature H_2O, we obtain $f_r = 0.026$ and slightly less for jet-cooled H_2O. In any case, almost all of the available energy is transferred into translational motion of the products:

$$f_t = 1 - f_r \approx 0.97\,. \quad (5)$$

The last equation is the simple consequence of the law of conservation of energy because the fraction of energy that is transferred into vibration is negligibly small, $f_v < 0.003$.

Based on the energy E_t released into translation, $E_t = f_t E_{av} = 124.7$ kJ/mol, the mean OH recoil velocity is calculated to be

$$\bar{v}_{OH} = (2E_t\mu)^{1/2}/m_{OH} = 900 \text{ m/s}, \quad (6)$$

where μ is the reduced mass of the H–OH system. This recoil velocity corresponds to a Doppler shift of

$$\Delta\nu_D = \nu\bar{v}_{OH}/c = 0.097 \text{ cm}^{-1} \quad (\text{at } 308 \text{ nm})\,.$$

For H_2O in the first absorption band, the photofragments will be ejected perpendicular to μ_{H_2O} the transition dipole moment of the parent. Therefore, a maximum Doppler width of $2\Delta\nu_D = 0.19$ cm^{-1} is expected. The bandwidth of the analyzing dye laser was $\Delta\nu_l = 0.1$ cm^{-1} in the UV. Therefore, no complete resolution of the OH absorption line was possible. Nevertheless, the measured absorption line width of 0.25 cm^{-1} fwhm confirms the expected value. Fig. 3 shows the recoil Doppler-broadened line

† A detailed discussion and evaluation of the alignment parameter $A_0^{(2)}$ is given in ref. [10].

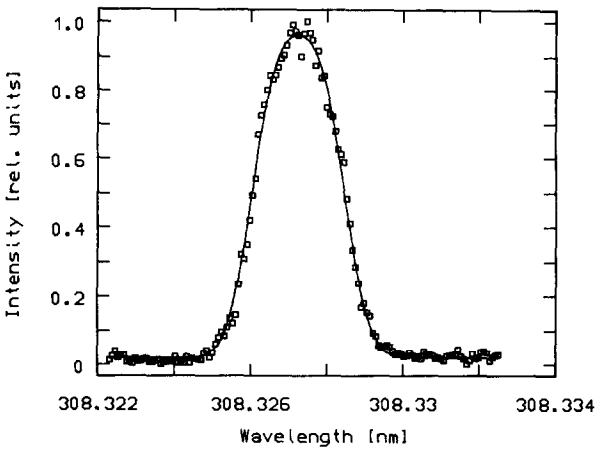

Fig. 3. High-resolution excitation spectrum around the $Q_1(4)$ transition. The linewidth of the dye laser is 0.1 cm^{-1} in the UV.

profile obtained for the $Q_1(4)$ line.

In general, the Doppler line-shape function $g(x_D)$ is given by

$$g(x_D) \sim [1+\beta_{eff}P_2(\cos\theta)P_2(x_D)]/2\Delta\nu_D\,, \qquad (7)$$

where $\Delta\nu_D$ is the maximum Doppler shift, $x_D=(\nu-\nu_0)/\Delta\nu_D$ is the relative displacement from the OH absorption line center ν_0, and $P_2(\cos\theta)$ is the second Legendre polynomial in $\cos\theta$. θ is the angle between E_D, the electric vector of the dissociating laser light, and the direction at which the fragment is probed. In the present experiment the propagation direction of the analyzing dye laser beam was perpendicular to E_D ($\theta=90°$)[‡]. The solid line in fig. 3 shows the best fitted profile $g(x_D)$ for a single recoil velocity of the OH fragments with a suitable convolution of a Gaussian profile to account for the probe laser linewidth ($\Delta\nu_l=0.1$ cm^{-1}) and parent Doppler motion ($\Delta\nu_{H_2O}=0.095$ cm^{-1}). The fitted anisotropy parameter, β_{eff}, is given by $\beta_{eff}=-0.4\pm0.3$. The negative value of β_{eff} confirms that the angular distribution is nearly a $\sin^2\theta$ distribution about the electric vector of the photolysis laser.

Table 1 shows a comparison of several dynamical parameters observed in the dissociation of H_2O at 157 and 193 nm. The main difference is the higher vibrational and rotational excitation of OH at the photolysis wavelength of 157 nm. The decrease of OH vibrational excitation with decreasing excitation energy can be explained by theoretical considerations [11]. An inspection of the $\tilde{A}\,^1B_1$ excited state surface can explain the low rotational excitation of the OH fragments. Since the photolysis wavelength of 193 nm is at the beginning of the H_2O absorption spectrum, the trajectories will start near the minimum of the upper surface, which is at a slightly larger OH bond length than in the equilibrium configuration of the ground state. At this configuration the $\tilde{A}\,^1B_1$ state has a minimum at bond angles near 105°. When the separation of a H atom starts, one of the two OH bond lengths in H_2O increases, and the angular dependence of the excited surface becomes weaker [2]. This does not significantly change the optimum bond angle. Therefore, only a negligible rotational excitation will be produced by final-state interaction.

The Boltzmann distribution of the OH rotational states can possibly be explained by a simple mapping of the parent molecule wavefunction onto the J_{OH} quantum number axis of the free OH radical [12]. For the lowest vibrational level of the parent molecule, the wavefunction is a Gaussian function of the

[‡] A detailed discussion and evaluation of the anisotropy parameter β_{eff} is given in ref. [10].

Table 1
Comparison of various dynamical parameters in the dissociation of H_2O following excitation of the $\tilde{X}\,^1A_1 \rightarrow \tilde{A}\,^1B_1$ transition at 157 nm [1] and 193 nm

Wavelength (nm)	E_{av}	f_T	f_v	f_r	$T_r(v''=0)$ (K)		$P_{v=1}/P_{v=0}$
					warm	jet[a]	
157	269.3	0.885	0.095	0.02	930	475	0.96
193	128.5	0.97	<0.003	0.03	400	300	<0.03

[a] Rotational temperature parameter T_r of jet-cooled H_2O is determined from the Q branch representing the Π^- component of the Λ doublet.

displacement coordinate (the H–O–H bending angle). If the upper potential surface essentially only brings about a separation between H– and –OH, then this Gaussian diatomic fragment rotational distribution can be characterized by a rotational temperature parameter.

Model calculations [13] have been used to characterize the photodissociation of a triatomic system. In the case of non-rotating H_2O, the mean rotational energy $\langle E_r \rangle_{OH}$ induced by the ν_3 vibration is given by

$$\langle E_r \rangle_{OH} = \tfrac{1}{8}\omega_3 \frac{m_O + m_H(1-\cos\varphi)}{m_{OH}}, \qquad (8)$$

where ω_3 is the energy of the bending vibrational mode ν_3, and $\varphi = 105°$ is the equilibrium H–O–H angle [14]. Eq. (8) yields a value of $\langle E_r \rangle_{OH} \approx 200$ cm^{-1}, which corresponds to a rotational temperature parameter of $T_r = 300$ K as observed in the experiment. For a quantitative comparison between theory and experiment finer details – such as the selective population of Λ components and the electronic structure of the products – become important [5]. The small increase in the OH rotational temperature, when room temperature H_2O is photolyzed, can be explained by a simple transformation of H_2O rotation into fragment rotation.

At 157 nm the situation is different. First, the OH rotational temperature is higher for jet cooled as well as for room temperature H_2O. This fact can be understood if different starting points for the trajectories are assumed. Moreover, it should be noted that the decrease in the OH rotational temperature from 930 to 475 K, on going from room-temperature to jet-cooled H_2O, is much greater than at 193 nm. This may indicate that the part of the excited surface which is sampled by rotationally excited H_2O at 157 nm is steeper than the part sampled at 193 nm.

Acknowledgement

We thank P. Andresen (Göttingen) for helpful discussions. Financial support from the Deutsche Forschungsgemeinschaft is gratefully acknowledged.

References

[1] P. Andresen and E.W. Rothe, J. Chem. Phys. 78 (1983) 989; P. Andresen, G.S. Ondrey and B. Titze, Phys. Rev. Letters 50 (1983) 486; P. Andresen, G.S. Ondrey, B. Titze and E.W. Rothe, J. Chem. Phys. 80 (1984) 2548.
[2] V. Staemmler and A. Palma, Chem. Phys. 93 (1985) 63.
[3] P. Andresen and E.W. Rothe, J. Chem. Phys. 82 (1985) 8634; P. Andresen, V. Benshausen, D. Häusler, H.W. Lülf and E.W. Rothe, J. Chem. Phys. 83 (1985) 1429.
[4] R. Schinke, V. Engel and V. Staemmler, Chem. Phys. Letters 116 (1985) 165; J. Chem. Phys. 83 (1985) 4522.
[5] R. Schinke, V. Engel, P. Andresen, D. Häusler and G.G. Balint-Kurti, Phys. Rev. Letters 55 (1985) 1180.
[6] H. Wang, W.S. Felps and S.P. McGlynn, J. Chem. Phys. 67 (1977) 2614.
[7] G.H. Dieke and H.M. Crosswhite, J. Quant. Spectry. Radiative Transfer 2 (1962) 97.
[8] W.L. Dimpfl and J.K. Kinsey, J. Quant. Spectry. Radiative Transfer 21 (1979) 233.
[9] M. Nuss, K.-H. Gericke and F.J. Comes, J. Quant. Spectry. Radiative Transfer 27 (1982) 191.
[10] K.-H. Gericke, S. Klee, F.J. Comes and R.N. Dixon, J. Chem. Phys. 86 (1986) 4463.
[11] V. Engel, R. Schinke and V. Staemmler, Chem. Phys. Letters 130 (1986) 413.
[12] R. Schinke and V. Engel, Faraday Discussions Chem. Soc. 82 (1986) paper 11.
[13] M.D. Morse and K.F. Freed, J. Chem. Phys. 78 (1983) 6045; M.D. Morse, Y.P. Band and K.F. Freed, J. Chem. Phys. 78 (1983) 6066.
[14] R. Vasudev, R.N. Zare and R.N. Dixon, J. Chem. Phys. 80 (1984) 4863.